Fermi National Accelerator Laboratory

FERMILAB-Conf-99/172-E
CDF

Dijet Results at CDF

F.S. Chlebana
For the CDF Collaboration

Fermi National Accelerator Laboratory
P.O. Box 500, Batavia, Illinois 60510

July 1999

Published Proceedings of the *7th International Workshop on Deep Inelastic Scattering and QCD,* Zeuthen, Germany, April 19-23, 1999

Dijet Results from CDF

F. S. Chlebana[a]

[a]Fermi National Accelerator Laboratory, P.O. Box 500, Batavia IL, 60150 U.S.A.

Recent dijet results from CDF are presented. The preliminary dijet mass distribution measured by CDF is presented and compared to QCD calculations. Measurements of dijet angular distributions are used to place limits on quark compositness. A preliminary measurement of the inclusive dijet differential cross section is presented.

1. Introduction

Jet production has proven to be a rich source of tests for QCD. Perturbative Next-to-Leading Order (NLO) and shower Monte Carlo calculations permit rapid calculation of many QCD jet processes with theoretical uncertainties small enough to allow detailed comparison with measured spectra [1]. Numerous parton distribution functions (PDFs) are available and provide an essential component of jet production calculations.

Measurements of the inclusive jet cross section from CDF have indicated an excess of events at high E_T when compared to the QCD predictions using standard PDFs [2]. Possible explanations range from quark substructure to an enhanced gluon distribution at high x.

In order to study this excess the dijet invariant mass distribution was measured and compared to theory predictions using different PDFs. Properties of parton-parton scattering can be studied by looking at dijet angular distributions. Such measurements are not strongly dependent on the choice of the PDF and are used to set limits on quark compositness [3]. By enhancing the gluon distribution at high x one can account for the rise in the jet cross section at high E_T. The triple differential dijet cross section covers a plane in x and Q^2 thus providing a sensitive constraint on the PDFs. This data will be useful as input to QCD fits to determine new sets of PDFs.

2. Dijet Mass

The preliminary CDF measurement of the differential dijet mass cross section is based on an integrated luminosity of 87 pb^{-1}. Events are collected using an inclusive E_T trigger with online thresholds of 20, 50, 70 and 100 GeV. The "snowmass" cone algorithm with $R \equiv \sqrt{\Delta\eta^2 + \Delta\phi^2} = 0.7$ is used to reconstruct the jets. The two leading jets are required to be within the central pseudorapidity, η, region and satisfy $|\eta| < 2$. Cuts were applied to reduce background and ensure a high trigger efficiency over the entire dijet mass range. The measured jet energies are corrected for detector and smearing effects. The dijet mass is determined from the standard 4-vector definition

$$M_{jj} = \sqrt{(E_1 + E_2)^2 - (\vec{p}_1 + \vec{p}_2)^2}, \qquad (1)$$

where E is the jet energy and $\vec{p}$ is the jet 3-momentum.

The results are plotted as (data-theory)/theory in the top plot of Figure 1 and compared with the predictions of JETRAD using different PDFs. The error bars represent the statistical error while the band represents the total systematic error. The CDF measurement is compared with the DØ results in the bottom plot [4]. The shape and normalization of the data from CDF and DØ are in agreement and consistent with QCD predictions.

3. Angular Distributions

Measurement of the distribution of the scattering angle between the dijet and proton beam, in the center-of-mass system, provides a fundamental test of QCD and is a sensitive probe of new physics. The distributions result from the dynamics of hard scattering of quarks and gluon-

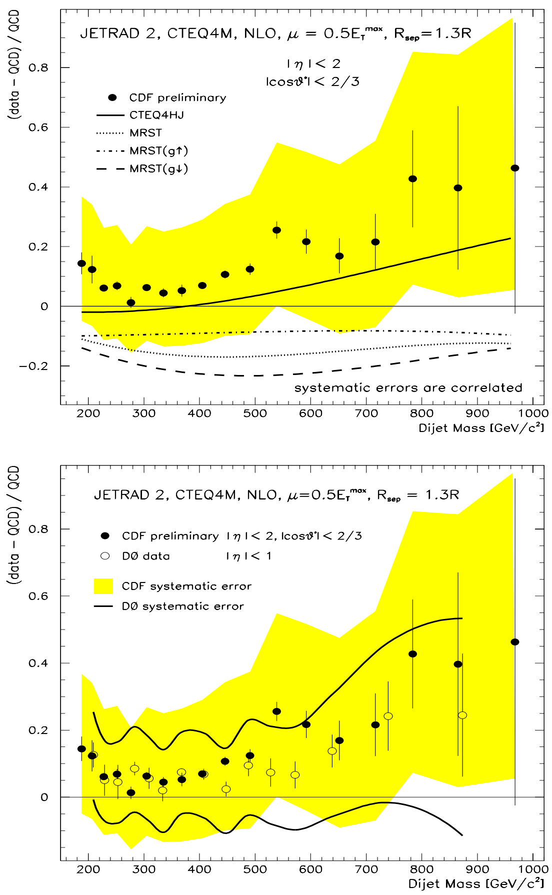

Figure 1. Top: The CDF dijet mass distribution compared with the prediction of JETRAD using different parton density functions. Bottom: CD-F (solid points) results compared with the DØ measurement (open points).

s and is expected to be fairly insensitive to the momentum distributions of the partons.

In order to allow an easier comparison with theory the angular distribution is plotted in the variable χ defined as

$$\chi = \frac{1+\cos\theta^*}{1-\cos\theta^*} = \mathrm{e}^{|\eta_1-\eta_2|}, \tag{2}$$

where θ^* is the center of mass scattering angle. The quantity χ uses only angles and is less sensitive to the energy scale of the detector. The

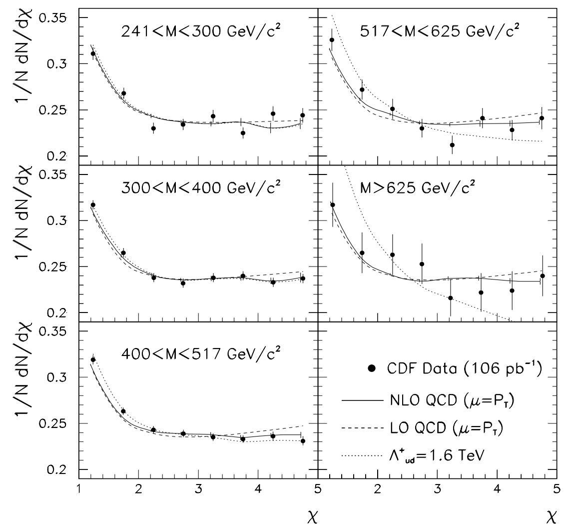

Figure 2. Dijet angular distributions for different mass bins.

results are plotted in Figure 2 for different mass bins.

The data excludes (at the 95% CL) a contact interaction scale of $\Lambda^+_{ud} \leq 1.6$ TeV and $\Lambda^-_{ud} \leq 1.4$ TeV. For a model where all quarks are composite $\Lambda^+ \leq 1.8$ TeV and $\Lambda^- \leq 1.6$ TeV.

4. Differential Dijet Cross Section

Preliminary results for the triple differential jet cross section, $d\sigma/(dE_T d\eta_1 d\eta_2)$ are presented by the CDF collaboration. The data set corresponds to an integrated luminosity of 86 pb^{-1}. The analysis includes events with at least two reconstructed jets. The *trigger* jet is required to satisfy $E_T > 40$ GeV and to be within the central η region, $0.1 < |\eta_1| < 0.7$. The *probe* jet is required to satisfy $E_T > 10$ GeV and to sit in one of four η bins, $0.1 < |\eta_2| < 0.7$, $0.7 < |\eta_2| < 1.4$, $1.4 < |\eta_2| < 2.1$ or $2.1 < |\eta_2| < 3.0$.

The well-understood response of the CDF central calorimeter is used to measure the E_T of the *trigger* jet. The measured energies are corrected for detector resolution and smearing using the same procedure as in the inclusive jet cross section measurement. The cross section is measured as a function of the trigger jet's E_T. Four separate distributions are determined corresponding to the four bins of η_2. Both jet combinations contribute to the distribution when there are two energetic central jets.

The preliminary results are compared to the NLO QCD calculation of JETRAD together with different PDFs in Figure 3. The error bars represent the statistical errors while the total systematic error is shown as a percentage below each plot.

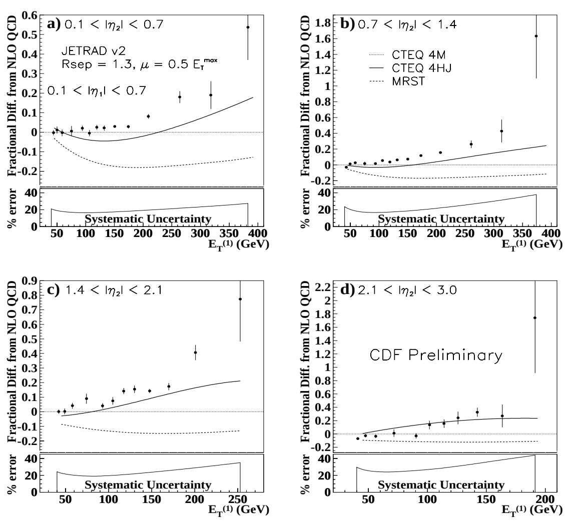

Figure 3. Triple differential dijet cross section.

The E_T and η of the leading jets are related to the momentum fraction, x, of the partons involved in the interaction. In leading order the relation is

$$x_1 = \frac{E_T}{\sqrt{s}}(\mathrm{e}^{\eta_1} + \mathrm{e}^{\eta_2}); \quad x_2 = \frac{E_T}{\sqrt{s}}(\mathrm{e}^{-\eta_1} + \mathrm{e}^{-\eta_2}). \tag{3}$$

For fixed E_T and η_1, different momentum fractions can be selected by requiring that the *probe* jet lie in different η intervals. We define $x_{\max}$ as the maximum of x_1 and x_2. For a two body process one intuitive choice for the QCD scale of the interaction is

$$Q^2 \sim -\hat{t} = 2E_T^2 \cosh^2 \eta^* (1 - \tanh \eta^*) \tag{4}$$

The data have been converted from (E_T, η_2) bins to $(x_{\max}, \hat{t})$ bins and shown in Figure 4. The high E_T region of the inclusive jet cross section distribution corresponds to high x.

The differential dijet cross section can be used as input to global QCD fits. We have seen that a modified gluon distribution can account for some of the excess of events observed at high E_T and expect that the extended $x - Q^2$ coverage of the dijet measurement will help constrain the shape of the PDFs when used in global QCD fits.

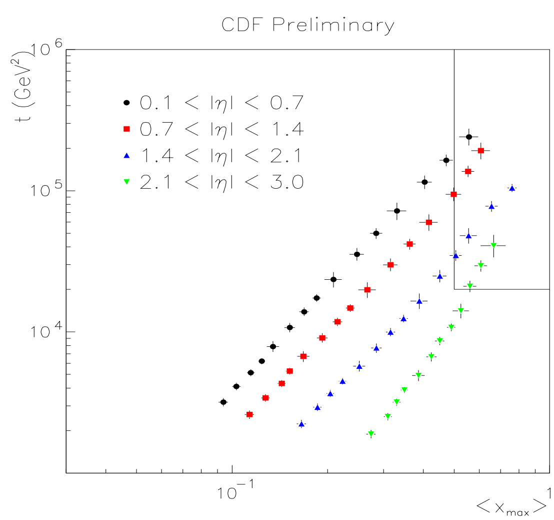

Figure 4. Region in $(x_{\max}, \hat{t})$ covered by the differential dijet cross section measurement.

REFERENCES

1. S. Ellis, Z. Kunszt and D. Soper, Phys. Rev. Lett. **64** 2121 (1990); W.T. Giele, E.W.N. Glover and D.A. Kosower, Nucl. Phys. **B403**, 633, (1993).
2. CDF Collab., F. Abe *et al.*, Phys. Rev. Lett. **77**, 438, (1996).
3. CDF Collab., F. Abe *et al.*, Phys. Rev. Lett. **77**, 5336, (1996).
4. DØ Collab., B. Abbott *et al.*, Phys. Rev. Lett. **82**, 2457, (1999).